

# Anomalous-magnetic-moment-enhanced Casimir effect

Daisuke Fujii<sup>1,2,\*</sup>, Katsumasa Nakayama<sup>3,†</sup> and Kei Suzuki<sup>1,‡</sup>

<sup>1</sup>Advanced Science Research Center, Japan Atomic Energy Agency (JAEA), Tokai, 319-1195, Japan

<sup>2</sup>Research Center for Nuclear Physics, Osaka University, Ibaraki 567-0048, Japan

<sup>3</sup>RIKEN Center for Computational Science, Kobe, 650-0047, Japan

We theoretically investigate the impact of the anomalous magnetic moment (AMM) of Dirac fermions on the fermionic Casimir effect under magnetic fields. We formulate it as an extension of the well-known Lifshitz formula. From our formula, we find that the AMM increases the fermionic Casimir energy. In particular, when the AMM is large enough, the Casimir energy is significantly enhanced by the gapless behavior of the lowest Landau level. We also quantitatively estimate the Casimir energy from electron, muon, and constituent quark fields under magnetic fields and propose possible phenomena at finite temperature and fermion density.

## I. INTRODUCTION

In 1948, Casimir predicted an attractive force working between parallel conducting plates, which is induced by a modification of the zero-point energy of photon fields in quantum electrodynamics (QED) vacuum [1]. About fifty years later, this effect was experimentally confirmed [2, 3] (see Refs. [4–11] for reviews). Nowadays, related phenomena are expected to be applied in the field of engineering, such as nanophotonics [10], where a significant issue is *how to control the Casimir effect through external environments*, such as temperature, density, and external fields. In this paper, we focus on magnetic fields.

The conventional Casimir effect (originating from the photon field) is hardly affected by magnetic fields because photons do not directly couple to magnetic fields [12],<sup>1</sup> whereas charged particles are directly affected. For example, Casimir effects originating from quantum fields under a magnetic field have been widely studied for charged scalar fields [16–32] as well as the Dirac field [20, 21, 25, 33–42]. As more realistic setup, one can consider fermionic Casimir effects inside thin films of Dirac/Weyl semimetals [38] and thin quark matter [42]. In these systems, the Casimir effect can be observed as change of thermodynamic quantities (e.g., pressure, specific heat, and magnetization) as a function of thickness, and one could control the Casimir effect by changing the strength of magnetic fields.

In the study of the Casimir effect under a magnetic field, a missing piece is the contribution of the anomalous magnetic moment (AMM) of charged fields. A representative example of AMM is a shift of the electron  $g$  factor from 2, which was calculated by Schwinger in 1948 [43, 44]. The role of AMM on the Casimir effect has never been studied in the prior studies [16–42]. As

a naive expectation, because a nonzero AMM modifies the eigenvalue spectrum (i.e., Landau levels) of charged particles, the AMM can also affect the property of the Casimir effect.

In this work, we investigate possible contributions of AMM on the Casimir effect. In QED, the AMM of electrons in vacuum or a weak magnetic field is usually tiny, but a strong magnetic field may induce a dynamical Zeeman effect (or dynamical AMM) [45, 46]. Also, in the low-energy region of quantum chromodynamics (QCD), up, down, and strange quarks have dynamical masses due to the spontaneous chiral symmetry breaking, and a part of their magnetic moments can be regarded as an AMM in the corresponding Dirac equation [47–49]. In the context of QCD phase diagram in magnetic fields, one can construct effective models based on constituent-quark degrees of freedom affected by such an AMM [50–72] (or Lorentz-tensor condensates [61, 67, 73–75], which leads to a similar but slightly different effect). Also in such situations, an AMM should play an important role of the magnetic response of Casimir effect.

This paper is organized as follows. In Sec. II, we formulate the Casimir effect from Dirac fields with AMM. In Sec. III, the typical behavior of the Casimir effect and numerical results are discussed. Section IV is devoted to the conclusion.

## II. FORMULATION

### A. Dirac field with AMM

In this work, we consider Dirac fields,  $\psi$  and  $\bar{\psi} \equiv \psi^\dagger \gamma_0$ , with a mass  $m$  and an electric charge  $q$ . As specific forms of electric charges,  $q_{e/\mu} = -e$  for the electron or the muon,  $q_u = \frac{2}{3}e$  for the up quark, and  $q_{d/s} = -\frac{1}{3}e$  for the down and strange quarks, where  $e > 0$  is the elementary charge.

The Lagrangian of the Dirac field is

$$\mathcal{L} = \bar{\psi}(i\gamma^\mu D_\mu - m + \frac{\kappa q}{2}\sigma^{\mu\nu}F_{\mu\nu})\psi, \quad (1)$$

where  $D_\mu \equiv \partial_\mu + iqA_\mu$  and  $F_{\mu\nu} = \partial_\mu A_\nu - \partial_\nu A_\mu$  are the covariant derivative and the field strength tensor

\* daisuke@rcnp.osaka-u.ac.jp

† katsumasa.nakayama@riken.jp

‡ k.suzuki.2010@th.phys.titech.ac.jp

<sup>1</sup> As another situation related to magnetic fields, one can consider the magnetic property of boundary conditions (e.g., [13–15]), but this is different from our purpose in our current study.

with an external U(1) gauge field  $A_\mu$ , respectively, and  $\sigma^{\mu\nu} = \frac{i}{2}(\gamma^\mu\gamma^\nu - \gamma^\nu\gamma^\mu)$ . The AMM is characterized by a parameter  $\kappa$ . When a magnetic field is applied in the  $z$  axis,  $\vec{B} = (0, 0, B)$ , and the Landau gauge  $A_\mu = (0, 0, Bx, 0)$  is chosen,

$$\mathcal{L} = \bar{\psi}(i\gamma^\mu D_\mu - m + \kappa q\sigma^{12}B)\psi. \quad (2)$$

By diagonalizing the Hamiltonian in momentum space, we obtain the dispersion relations [76]:

$$\omega_{l,s} = E_{l,s}, \quad (3)$$

$$\tilde{\omega}_{l,s} = -E_{l,s}, \quad (4)$$

where

$$E_{l,s} = \sqrt{k_z^2 + \left(\sqrt{m^2 + (2l+1-s\zeta)|qB|} - s\kappa qB\right)^2}, \quad (5)$$

which is labeled by the quantum number of discrete levels  $l = 0, 1, 2, \dots$ , the spin  $s = \pm 1$ , and  $\zeta = \text{sgn}(qB)$ . When we set  $\zeta = +1$ , the lowest modes are the set of  $\omega_{l=0,+}$  and  $\tilde{\omega}_{l=0,+}$ . We call this set the *lowest Landau levels (LLs)*, and the other levels *higher Landau levels (HLLs)*.

Typical examples of the  $\kappa$ -dependence of dispersion relations in a fixed  $qB = m^2$  are shown in Fig. 1.

- (i) At  $\kappa = 0$ , the LLs are spin-projected, whereas the HLLs are doubly degenerate between e.g.,  $\omega_{l=0,-}$  and  $\omega_{l=1,+}$ , which is a well-known feature of the Dirac field under magnetic fields [77, 78] (see the black dashed lines in Fig. 1).
- (ii) At  $\kappa \neq 0$ , we can see that a nonzero AMM splits the spin degeneracy of HLLs, and the gap of the LLL, characterized by the mass  $m$ , gets smaller [see Fig. 1(a)].
- (iii) At a critical AMM  $\kappa^{\text{cri}(0)} = m/qB$  which we call the *lowest critical AMM*, the LLs becomes a linear dispersion relation due to the cancellation of the mass and the AMM [79, 80] [see the red solid lines in Fig. 1(b)].
- (iv) At a larger  $\kappa > m/qB$ , the gap of the LLs become is opened again, whereas the gap of the first LLs (i.e.,  $l = 1$ ) decreases with increasing  $B$ .
- (v) At  $\kappa^{\text{cri}(1)} = \sqrt{m^2 + 2|qB|}/qB$  which we call the *first critical AMM*, the gap of the first LLs vanishes, and the linear dispersion relations appears [see the blue solid lines in Fig. 1(c)].
- (vi) At a larger  $\kappa > \sqrt{m^2 + 2|qB|}/qB$ , and the first LLs become gapped again.
- (vii) This series of behaviors holds for any  $l$ , where each critical AMM is  $\kappa^{\text{cri}(l)} = \sqrt{m^2 + 2l|qB|}/qB$ .

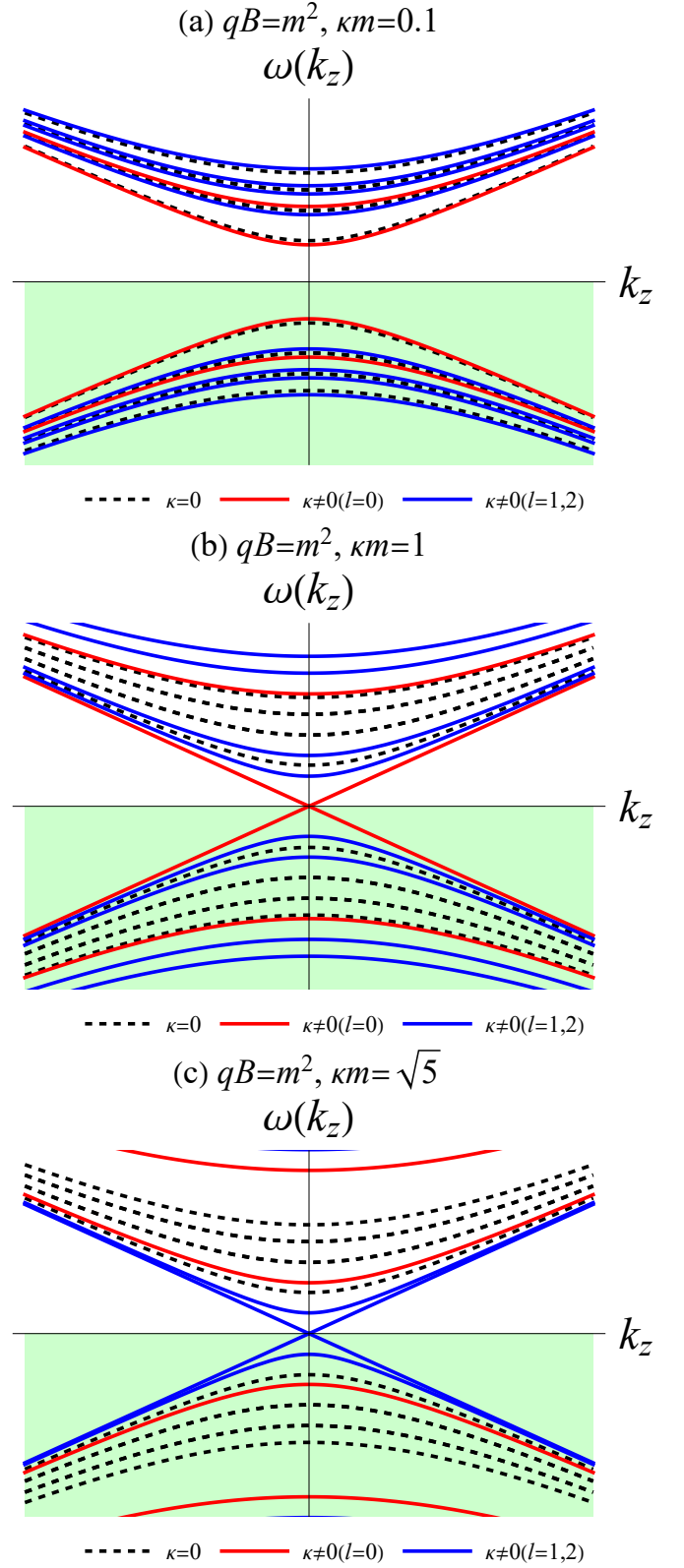


FIG. 1. Examples of dispersion relations in massive Dirac fields in a fixed magnetic field at (a) a small  $\kappa$ , (b) the lowest critical AMM  $\kappa^{\text{cri}(0)}$ , and (c) the first critical AMM  $\kappa^{\text{cri}(1)}$ .

(viii) We note that, this sequence occurs also when we vary the magnetic field at a fixed  $\kappa$  [80], where the critical magnetic field for the LLLs is  $qB^{\text{cri}(0)} = m/\kappa$ . In the following analysis, we will focus on this magnetic field as a typical parameter, and we simply denote it by  $qB^{\text{cri}} \equiv qB^{\text{cri}(0)}$ .

### B. Zero-point energy

Using the dispersion relations, the thermodynamic potential  $\Omega \equiv -\frac{T}{V} \ln Z$  (per unit volume  $V = L_x L_y L_z$  at a temperature  $T = 1/\beta$  with the distribution function  $Z$ ) is

$$\Omega = -\frac{|qB|}{2\pi} \int \frac{dk_z}{2\pi} \sum_{l,s} \left[ \frac{1}{2} |\omega_{l,s}| + \frac{1}{2} |\tilde{\omega}_{l,s}| + \frac{1}{\beta} \ln \left\{ \left(1 + e^{-\beta|\omega_{l,s}|}\right) \left(1 + e^{-\beta|\tilde{\omega}_{l,s}|}\right) \right\} \right], \quad (6)$$

where the overall minus sign is a property of fermions. The factor of  $|qB|/2\pi$  is called the Landau degeneracy factor, which is obtained from the momentum integral  $\int dk_x dk_y / (2\pi)^2$  at  $B = 0$ . By taking the zero-temperature limit of Eq. (6), we obtain the zero-point energy of the system:

$$\begin{aligned} \Omega(T \rightarrow 0) &= -\frac{|qB|}{2\pi} \int \frac{dk_z}{2\pi} \sum_{l,s} \left( \frac{1}{2} |\omega_{l,s}| + \frac{1}{2} |\tilde{\omega}_{l,s}| \right) \\ &\equiv \frac{E_0^{\text{int}}}{L_z}. \end{aligned} \quad (7)$$

Note that we defined  $E_0^{\text{int}}$  as the zero-point energy per unit area  $L_x L_y$  (i.e., an energy surface density), and its mass dimension is 3.

### C. Casimir energy

To discuss the Casimir energy, we consider the zero-point energy in a finite volume. In this work, we impose the periodic boundary conditions (PBCs)<sup>2</sup> at  $z = 0$  and  $z = L_z$  in the  $z$  direction,<sup>3</sup> where the spatial momentum is discretized as  $k_z = 2n\pi/L_z$  ( $n = 0, \pm 1, \pm 2, \dots$ ). Then, using the replacements of  $L_z \int dk_z / 2\pi \rightarrow \sum_n$ ,  $\omega_{l,s} \rightarrow \omega_{l,s,n}$ , and  $\tilde{\omega}_{l,s} \rightarrow \tilde{\omega}_{l,s,n}$  in Eq. (7), the zero-point energy (per unit area) at finite  $L_z$  is

$$E_0^{\text{sum}} \equiv -\frac{|qB|}{2\pi} \sum_{l,s} \sum_{n=-\infty}^{\infty} \left( \frac{1}{2} |\omega_{l,s,n}| + \frac{1}{2} |\tilde{\omega}_{l,s,n}| \right). \quad (8)$$

This infinite sum (8) has an ultraviolet divergence. To get the finite Casimir energy, we need a regularization scheme.

The Lifshitz formula is a powerful tool, which was first derived for calculating the conventional photonic Casimir energy by Lifshitz [81]. The corresponding formula for the Dirac field in a nonzero magnetic field was used in Ref. [42], which is equivalent to the result derived from other regularization schemes (e.g., the proper-time regularization [33, 34], the Abel-Plana formula [21], the zeta-function regularization [35], and the lattice regularization [42]).

In this work, we apply the Lifshitz formula with an AMM:

$$\begin{aligned} E_{\text{Cas}} &= -2 \int_{-\infty}^{\infty} \frac{d\xi}{2\pi} \sum_{l,s} \frac{|qB|}{2\pi} \ln \left[ 1 - e^{-L_z \tilde{k}_z^{[l,s]}} \right], \quad (9) \\ \tilde{k}_z^{[l,s]} &= \sqrt{\left( \sqrt{m^2 + (2l+1-s\zeta)|qB| - s\kappa qB} \right)^2 + \xi^2}. \end{aligned}$$

This is the main formula in the current work. The overall factor  $-2$  is the minus sign of the fermion zero-point energy and the factor due to the PBC. The integral variable  $\xi$  is the imaginary part of the imaginary energy, where the integral over  $\xi$  covers the contributions of the particle and antiparticle degrees of freedom. At  $\kappa = 0$ , this formula is reduced to the formula used in Ref. [42].<sup>4</sup>

## III. RESULTS

### A. Typical behaviors

Figure 2 shows the  $\kappa$  dependence ( $\kappa m = 0, 0.01, 0.1, 0.5, 1$ ) of the Casimir energy in a fixed magnetic field  $qB = m^2$ . Here, we plot a Casimir coefficient

$$C_{\text{Cas}}^{[1]} \equiv L_z E_{\text{Cas}}, \quad (10)$$

where the superscript [1] denotes the power of  $L_z$  in the right-hand side. This quantity is useful for focusing on the  $1/L_z$  scaling behavior. In the longer- $L_z$  region, the Casimir energy is dominated by the LLLs, because they are the lightest among all LLs within the current parameters. From Fig. 2, we find that a nonzero  $\kappa$  leads to an enhancement of the Casimir energy. This increase is caused by the reduction of the energy gaps of the LLLs in the dispersion relations. In particular, at the critical AMM ( $m\kappa = 1$ ), the Casimir energy  $E_{\text{Cas}}$  has a clear

<sup>2</sup> Within our regularization scheme, it is also straightforward to derive the formula under the antiperiodic boundary conditions.

<sup>3</sup> This setup is easy because  $k_z$  is a conserved quantity in systems under a magnetic field, whereas the case with boundary conditions imposed in the  $x$  or  $y$  direction is analytically difficult.

<sup>4</sup> Precisely speaking, we need substitute  $b = \mu = 0$  and remove  $N_c \sum_{q_f}$  in Eq. (11) of Ref. [42]. Note that there are two ways to assign indices of Landau levels: the two modes  $\omega_{l=0,+}$  and  $\omega_{l=0,-}$  assigned in this work are written as  $\omega_{l=0}$  and either of  $\omega_{l=1,\pm}$  in Ref. [42], respectively.

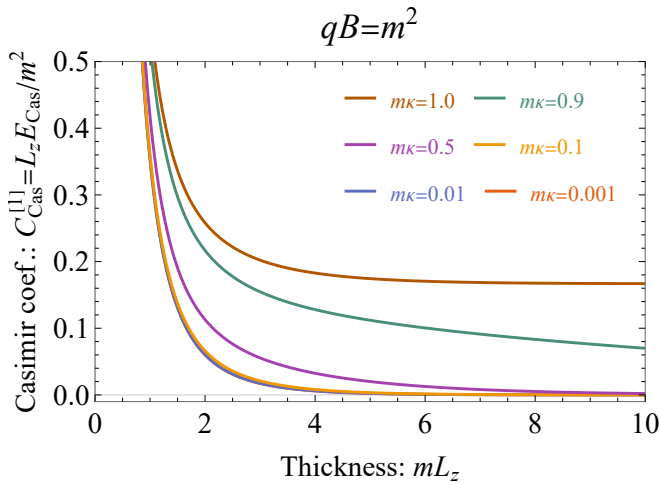


FIG. 2. Casimir coefficient  $C_{\text{Cas}}^{[1]} \equiv L_z E_{\text{Cas}}$  without ( $\kappa = 0$ ) and with AMM ( $\kappa \neq 0$ ).

$1/L_z$  scaling, which is a typical feature for gapless dispersions. This is one of our main findings in this work: when the AMM is large enough, the LLLs become effectively gapless, which results in a significant enhancement of the Casimir energy. We note that the gapless dispersion also occurs even when the magnetic field is strong enough at a fixed AMM [79, 80], where the critical magnetic field is  $qB^{\text{cri}} = m/\kappa$ . Therefore, even if the AMM is small, a strong magnetic field can significantly enhance the Casimir effect.

On the other hand, when the AMM is smaller compared to the mass ( $m\kappa < 1$ ), the long- $L_z$  behavior is strongly suppressed, which is a nonzero-mass effect characterized by  $m \neq 0$  and a well-known behavior for massive fields [82–84].

In the shorter- $L_z$  region of Fig. 2, the Casimir energy increases, which indicates an enhancement stronger than the  $1/L_z$  scaling. This is because the higher LLs (as well as the LLLs) contribute to the Casimir effect. We find that, also in this region, the Casimir energy is enhanced by the AMM.

Next, to examine the significance of the AMM effect, we define the Casimir energy difference at  $\kappa \neq 0$  and  $\kappa = 0$  as

$$\Delta E_{\text{Cas}} \equiv E_{\text{Cas}}(\kappa) - E_{\text{Cas}}(\kappa = 0). \quad (11)$$

A semi-log plot is useful for examining *exponential scaling behavior* in the long- $L_z$  region. In Fig. 3, we find that  $\Delta E_{\text{Cas}}$  behaves linearly in the long- $L_z$  region  $mL_z > 1$ . This indicates that  $\Delta E_{\text{Cas}}$  decays exponentially in this region. At larger  $\kappa$  ( $m\kappa = 0.5$ ), the slope of linear behavior is determined by both  $m$  and  $\kappa$ :  $\Delta E_{\text{Cas}} \propto e^{-(m-\kappa|qB|)L_z}$ . At smaller  $\kappa$  ( $m\kappa = 0.001, 0.01, 0.1$ ), the slope is mostly determined by  $m$  and the  $\kappa$  dependence is suppressed: the exponential scaling in this region is  $\Delta E_{\text{Cas}} \propto e^{-mL_z}$ . These scaling laws arise from the LLL dominance in

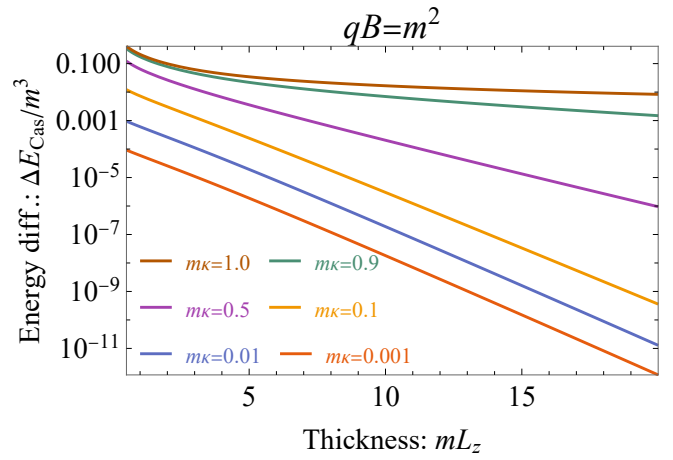


FIG. 3. Semi-log plot of Casimir energy enhancement  $\Delta E_{\text{Cas}}$  due to  $\kappa \neq 0$ .

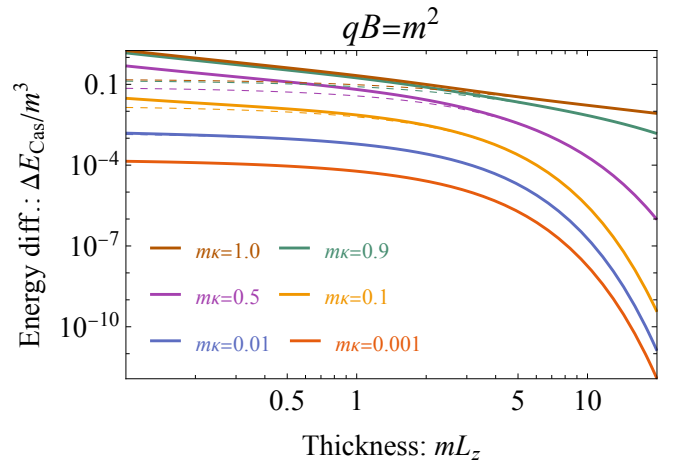


FIG. 4. Log-log plot of Casimir energy enhancement  $\Delta E_{\text{Cas}}$  due to  $\kappa \neq 0$ . Solid lines: the results with the LLLs and HLLs. Dashed lines: with only LLLs.

the long  $L_z$  region.<sup>5</sup> Note that, near the critical AMM ( $m\kappa \sim 1$ ),  $\Delta E_{\text{Cas}} \propto 1/L_z$ , which is not exponential scaling.

A log-log plot is useful for focusing on the short- $L_z$  region and also examining the *power-law scaling behavior* of a physical quantity. In Fig. 4, we find that  $\Delta E_{\text{Cas}}$  behaves linearly at a short  $L_z$  (now,  $mL_z \lesssim 2$ ), which is the power-law scaling. In addition, in this region, we

<sup>5</sup> An expression of the Casimir energy for the LLLs, which is equivalent to the  $l = 0$  term in Eq. (9), is given as

$$E_{\text{Cas,LLL}} = \frac{|qB|}{2\pi} \times \frac{2M}{\pi} \sum_{j=1}^{\infty} \frac{K_1[jML_z]}{j}, \quad (12)$$

where  $K_1$  is the modified Bessel function, and  $M = m - \kappa|qB|$  within  $M > 0$ . By focusing on the  $j = 1$  term and using  $K_1(x) \approx \sqrt{\frac{\pi}{2x}} e^{-x}$  for  $x \gg 1$ , we can get an exponential-type function.

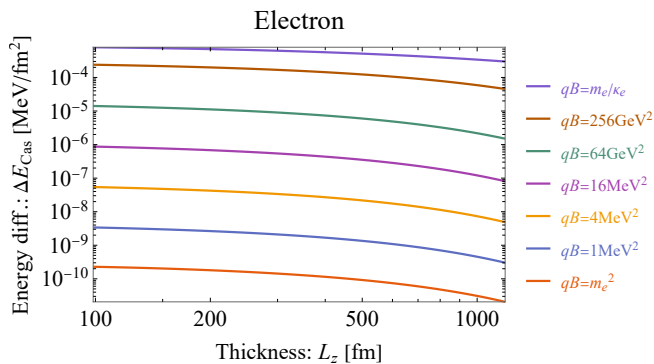


FIG. 5. Casimir energy enhancement  $\Delta E_{\text{Cas}}$  for electrons.

can examine the contribution of each LL. The dashed lines in Fig. 4 represent the results with only the LLLs. We find that, at larger  $\kappa$ , the HLLs (as well as the LLLs) contribute to the enhancement of the Casimir energy. On the other hand, at smaller  $\kappa$ , the LLLs are still dominant.

### B. Electrons

Next, we discuss the Casimir energy from the electron field in the QED vacuum. In zero magnetic field, the intrinsic AMM is a well-known value  $a \equiv (g - 2)/2 = \alpha/2\pi$  in the one-loop level, which was derived by Schwinger [43, 44]. A nonzero magnetic field induces an additional AMM. Within the perturbation theory in the first order of  $\alpha$ , the induced AMM tends to weaken the intrinsic AMM  $\alpha/2\pi$  in both the weak and strong magnetic fields [85–92]. However, it can be nonperturbatively enhanced by a strong magnetic field [45, 46]. In this section, for simplicity, we input  $\alpha/2\pi$ .

By substituting the experimental values [93],  $a_e = 0.00115965218062$  and  $m_e = 0.51099895000$  MeV, into  $\kappa \equiv a/2m$ , we obtain

$$\kappa_e = 0.00113469 \text{ MeV}^{-1}. \quad (13)$$

By inputting these parameters into Eq. (9), we can estimate the Casimir energy.<sup>6</sup>

The numerical results are shown in Fig. 5, where we show a wide range of magnetic fields from  $qB = m_e^2 \sim 0.25 \text{ MeV}^2$  (i.e., the Schwinger limit) to the critical magnetic field  $qB^{\text{cri}} = m_e/\kappa_e \sim 450 \text{ MeV}^2$ . From this figure, we find that the Casimir energy is enhanced with increasing magnetic field. For example, at  $qB = m_e^2$ , the enhancement is  $\Delta E_{\text{Cas}} \sim 2.3 \times 10^{-10} \text{ MeV/fm}^2$  at  $L_z = 100 \text{ fm}$ . At the critical field  $qB^{\text{cri}}$ ,  $\Delta E_{\text{Cas}} \sim 7.9 \times 10^{-4} \text{ MeV/fm}^2$  at  $L_z = 100 \text{ fm}$ .

<sup>6</sup> The magnetic-field dependence of the parameters,  $m_e$  and  $\kappa_e$ , is omitted to simplify the interpretation of the results.

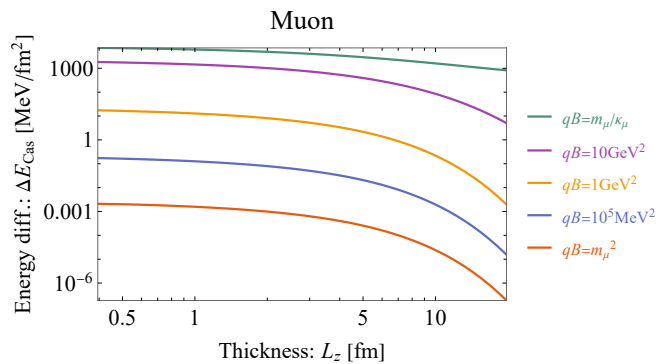


FIG. 6. Casimir energy enhancement  $\Delta E_{\text{Cas}}$  for muons.

### C. Muons

The case of muons is similar to that of electrons. By substituting the experimental values [93],  $a_\mu = 0.00116592059$  and  $m_\mu = 105.6583755$  MeV, into  $\kappa \equiv a/2m$ , we obtain

$$\kappa_\mu = 5.51741 \times 10^{-6} \text{ MeV}^{-1}. \quad (14)$$

The results are shown in Fig. 6, where we show a wide range of magnetic fields from  $qB = m_\mu^2 \sim 1.1 \times 10^4 \text{ MeV}^2$  to the critical magnetic field  $qB^{\text{cri}} = m_\mu/\kappa_\mu \sim 19 \text{ GeV}^2$ . We find that the enhancement of the Casimir energy of muons is smaller than that of electrons at the same magnetic field. Therefore, a significant enhancement is induced by stronger magnetic fields. For example, at  $qB = m_\mu^2$ , the enhancement is  $\Delta E_{\text{Cas}} \sim 1.57 \times 10^{-3} \text{ MeV/fm}^2$  at  $L_z = 1 \text{ fm}$ . At the critical field  $qB^{\text{cri}}$ ,  $\Delta E_{\text{Cas}} \sim 6100 \text{ MeV/fm}^2$  at  $L_z = 1 \text{ fm}$ .

### D. Constituent quarks

Contrary to the AMMs of electrons and muons, the AMMs of constituent quarks are nontrivial because they are not gauge-invariant. However, it is useful in an effective quark model analysis, such as the study of the phase diagram in the Nambu–Jona-Lasinio (NJL) model [94, 95]. Therefore, at least, our following analysis will be useful for the investigation of the Casimir effect originating from constituent quark fields as degrees of freedom in an effective quark model. In addition, the AMMs of constituent quarks are related to the magnetic moments of hadrons, and such an AMM-induced effect is interesting also in the context of the hadronic Casimir effect.<sup>7</sup>

<sup>7</sup> In addition, the Casimir effect in the deconfined phase of QCD is induced by not only quark fields but also gluon fields. Lattice numerical simulations are powerful for investigating such a gluonic Casimir effect [96–99].

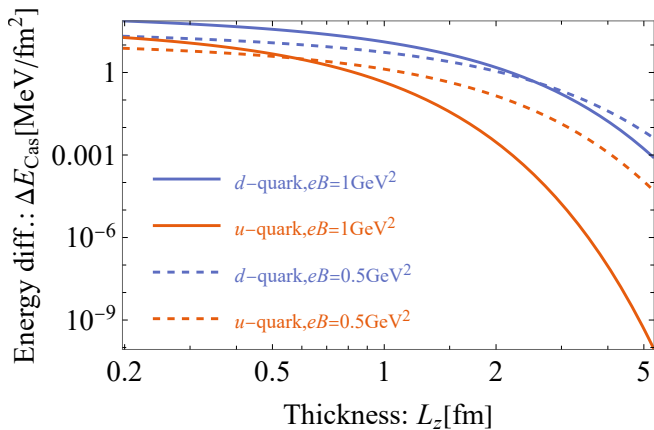


FIG. 7. Casimir energy enhancement  $\Delta E_{\text{Cas}}$  for constituent  $u, d$  quarks.

In studies of the phase diagram in the NJL model [50–72], the quark AMM can be introduced in several approaches: (i) a constant AMM [50–58, 60, 62–65, 67, 68, 70, 72], (ii) an AMM proportional to the chiral condensate (i.e.,  $\kappa \propto \sigma$  with the  $\sigma$  mean field) [53, 59, 61, 62], or (iii) an AMM proportional to the square of the chiral condensate (i.e.,  $\kappa \propto \sigma^2$ ) [61, 62, 66, 69, 71]. Such assumptions enable systematic investigations of how the phase diagram responds to different treatments of the AMM.

In this work, under the scenario of approach (i), we adopt an estimate based on the framework of the constituent quark model, proposed in Refs. [48, 50]. By inputting the experimental values of baryon masses and magnetic moments, we obtain (see Appendix A),

$$\kappa_u = 0.00952827 \text{ GeV}^{-1}, \quad (15)$$

$$\kappa_d = 0.0831157 \text{ GeV}^{-1}. \quad (16)$$

By substituting these AMM parameters into the gap equation in the NJL model, we can evaluate the constituent quark masses modified by an external magnetic field (see Appendix B). By inputting the constituent quark masses and the AMM parameters into Eq. (9) and multiplying the factor of the number of colors  $N_c = 3$ , we can calculate the Casimir energy for the constituent  $u$  and  $d$  quarks.<sup>8</sup>

In Fig. 7, we show the results at  $eB = 0.5$  and  $1 \text{ GeV}^2$ . We find that the enhancement of the Casimir energy for the  $d$  quark is larger than for the  $u$  quark. This is because the AMM of the  $d$  quark is larger than that of the  $u$  quark. Quantitatively, the energy scale of Casimir energy is similar to that of muons, shown in the previous section. This is because the effective masses of constituent quarks are similar to the muon mass  $m_\mu \sim 100 \text{ MeV}$ .

<sup>8</sup> As a more advanced analysis, it is straightforward to implement the  $L_z$  dependence in the gap equation, while we omit it to simplify the interpretation of the results.

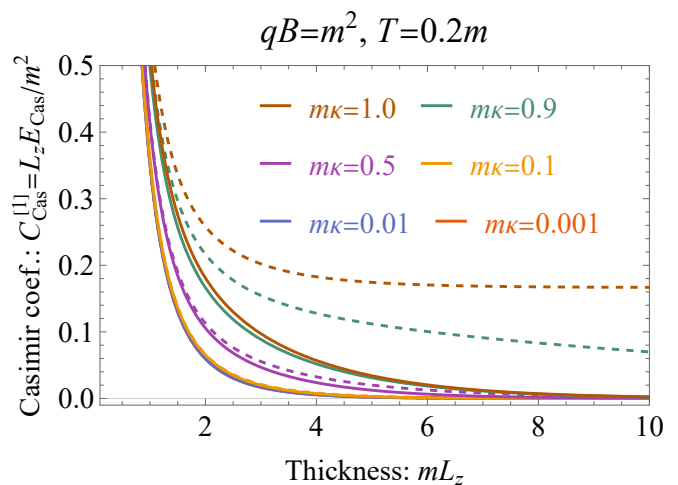


FIG. 8. Casimir coefficient  $C_{\text{Cas}}^{[1]} \equiv L_z E_{\text{Cas}}$  without ( $\kappa = 0$ ) and with AMM ( $\kappa \neq 0$ ) at finite temperature  $T = 0.2m$ . The dashed lines are at  $T = 0$ , which is the same as Fig. 2.

In addition, we note that, in the long- $L_z$  region, the Casimir energy (and its enhancement due to the AMM) at  $eB = 1 \text{ GeV}^2$  is smaller than the result at  $eB = 0.5 \text{ GeV}^2$ . This is because larger magnetic fields induce heavier dynamical masses. Thus, the magnetic field does not necessarily enhance the Casimir energy, and a dynamical mass generation can suppress the Casimir energy.

### E. At finite temperature

Next, we consider the situation at finite temperature  $T$ . In Eq. (9), using the replacement of  $\int_{-\infty}^{\infty} \frac{d\xi}{2\pi} f(\xi) \rightarrow T \sum_{\mathcal{N}=-\infty}^{\infty} f(\xi_{\mathcal{N}})$ , where  $\xi_{\mathcal{N}} = (2\mathcal{N} + 1)\pi T$  is the fermionic Matsubara frequency, we can obtain the corresponding Lifshitz formula:

$$E_{\text{Cas}} = -2T \sum_{\mathcal{N}=-\infty}^{\infty} \sum_{l,s} \frac{|qB|}{2\pi} \ln \left[ 1 - e^{-L_z \tilde{k}_z^{[l,s]}} \right], \quad (17)$$

$$\tilde{k}_z^{[l,s]} = \sqrt{\left( \sqrt{m^2 + (2l+1-s\zeta)|qB|} - s\kappa qB \right)^2 + \xi_{\mathcal{N}}^2}.$$

As a typical behavior at finite temperature, Fig. 8 shows the results at  $T = 0.2m$ . We find that the temperature effect suppresses the long  $L_z$ -behavior in the Casimir energy, which is a general feature in the case of the fermion fields (i.e., the effective gap effect due to the fermionic Matsubara frequency). Therefore, the enhancement of the Casimir energy due to the AMM can be affected by finite temperature.

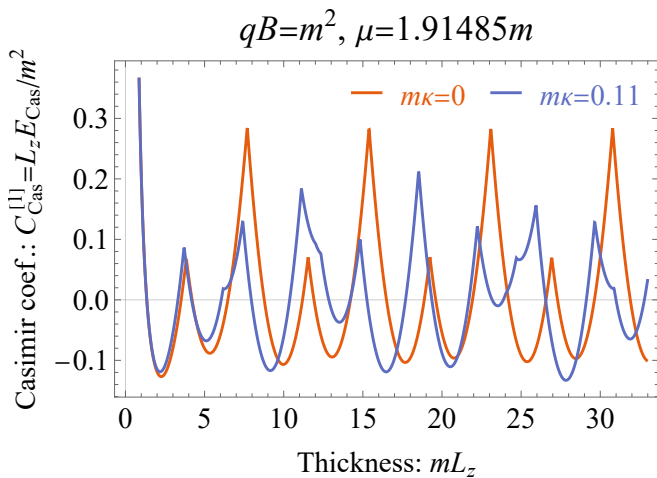


FIG. 9. Casimir coefficient  $C_{\text{Cas}}^{[1]} \equiv L_z E_{\text{Cas}}$  without ( $\kappa = 0$ ) and with AMM ( $\kappa \neq 0$ ) at finite density  $\mu = 1.91485m$ .

### F. At finite density

Finally, we discuss a possible impact of AMM on the Casimir effect at finite fermion chemical potential or fermion density. For studies about Dirac-fermion matter with AMM under magnetic field, see, e.g., Refs. [80, 100, 101]. The situation we consider can be realized when the size of materials consisting of fermions is extremely thin, e.g., in electron gas confined inside a thin cavity or a thin size of quark matter.<sup>9</sup> At finite chemical potential  $\mu$ , the dispersion relations are

$$\omega_{l,s} = E_{l,s} - \mu, \quad (18)$$

$$\tilde{\omega}_{l,s} = -E_{l,s} - \mu, \quad (19)$$

where  $E_{l,s}$  is the same as Eq. (5). The corresponding Lifshitz formula is

$$E_{\text{Cas}} = -2 \int_{-\infty}^{\infty} \frac{d\xi}{2\pi} \sum_{l,s} \frac{|qB|}{2\pi} \ln \left[ 1 - e^{-L_z \tilde{k}_z^{[l,s]}} \right], \quad (20)$$

$$\tilde{k}_z^{[l,s]} = \sqrt{\left( \sqrt{m^2 + (2l+1-s\zeta)|qB|} - s\kappa qB \right)^2 - (i\xi + \mu)^2}.$$

This formula includes both the contributions from the Dirac-fermion vacuum and the finite-density environment. When  $\mu = 0$ , this formula reduces to Eq. (9).

In Fig. 9, we compare results at finite density with  $\kappa = 0$  and  $\kappa \neq 0$ , where the parameters are adjusted such that the Fermi level crosses the three modes of  $\omega_{l=0,+}$ ,  $\omega_{l=0,-}$ , and  $\omega_{l=1,+}$ . It is known that when an energy level crosses the Fermi level, the Casimir energy oscillates as a

function of  $L_z$ , and its period is determined by the Fermi momentum [42, 102, 103]. At  $\kappa = 0$ , the lowest state is the LLL  $\omega_{l=0,+}$ , and the second-lowest states,  $\omega_{l=0,-}$  and  $\omega_{l=1,+}$ , are doubly degenerate. Then, the Casimir energy oscillates, which is characterized by two oscillation periods,  $mL_z^{\text{osc}} \sim 3.85$  and  $7.70$ . On the other hand, at  $\kappa \neq 0$ ,  $\omega_{l=0,-}$  and  $\omega_{l=1,+}$  are split by the AMM. Then, the oscillation of the Casimir energy is characterized by three oscillation periods. Thus, a nonzero AMM can induce a new oscillation period by the level splitting between two modes. In other words, the presence of multiple oscillation periods can be evidence of the AMM.

Note that in Fig. 9, we have focused on the situation with the three Landau levels, but in principle, this discussion holds even when more Landau levels cross the Fermi level.

## IV. CONCLUSION

In this paper, we have discussed the impact of AMM on the Casimir effect originating from Dirac-fermion fields under a magnetic field. From the main formula, Eq. (9), we have found the following features:

1. *Casimir energy enhancement*—The Casimir energy in the long- $L_z$  region is enhanced by a nonzero AMM. This is because the Casimir energy in this region is dominated by the LLLs, and the lower energy shift of the LLL increases the Casimir energy.
2. *Enhancement from HLLs*—The Casimir energy in the short- $L_z$  region is also enhanced by a nonzero AMM, where the Casimir energy is dominated by the sum of HLLs as well as the LLLs.
3. *Significant enhancement from gapless LLs*—When the AMM (and/or the magnetic field) is large enough, the Casimir energy significantly increases. This is because the dispersion relations of the LLLs become an effectively gapless form.

Thus, the enhancement of the Casimir energy is a robust property in many cases of Dirac fields. This feature will be useful for controlling the fermionic Casimir effect by magnetic fields.

## ACKNOWLEDGMENTS

The authors thank Mamiya Kawaguchi for fruitful discussions about quark AMMs. This work was supported by the Japan Society for the Promotion of Science (JSPS) KAKENHI (Grants No. JP24K07034, JP24K17054, JP24K17059).

<sup>9</sup> Note that Casimir effects with the PBC are not unphysical. The PBC is useful for investigating the Casimir effect not only in lattice numerical simulations but also in winding geometries such as nanorings, nanotubes, and solid tori.

## Appendix A: Magnetic moments of constituent quarks

In Subsection III D, the AMMs of constituent quarks were used as input parameters. In this Appendix, we estimate the AMMs of constituent quarks based on the method proposed in Refs. [48, 50]. In our analysis, the most recent values in the Particle Data Group [93] are used as input parameters. The experimental values for the magnetic moments for the proton, neutron, and  $\Lambda$  baryon are [93]

$$\mu_p = 2.7928473446 \mu_N, \quad (\text{A1})$$

$$\mu_n = -1.9130427 \mu_N, \quad (\text{A2})$$

$$\mu_\Lambda = -0.613 \mu_N, \quad (\text{A3})$$

respectively, where  $\mu_N \equiv \frac{e}{2m_p}$  is the nuclear magneton with the elementary charge  $e$  and the proton mass  $m_p$ . In the constituent quark model [104], the magnetic moments of the constituent quarks are expressed as

$$\mu_u = \frac{4\mu_p + \mu_n}{5} = 1.85167 \mu_N, \quad (\text{A4})$$

$$\mu_d = \frac{\mu_p + 4\mu_n}{5} = -0.971865 \mu_N, \quad (\text{A5})$$

$$\mu_s = \mu_\Lambda = -0.613 \mu_N. \quad (\text{A6})$$

Here, we define the magnetic moments of constituent quarks as  $\mu_f = \frac{\bar{q}_f e}{2M_f} (1 + a_f)$ , where the quark flavor is labeled by  $f = u, d, s$ ,  $M_f$  is the constituent quark mass, and the magnitudes of electric charges are  $\bar{q}_u = 2/3$  and  $\bar{q}_d = \bar{q}_s = -1/3$ . Then, we obtain the following expression for the constituent-quark AMM:

$$a_f = \frac{2M_f \mu_f}{\bar{q}_f e} - 1 = \frac{M_f \mu_f}{\bar{q}_f m_p \mu_N} - 1, \quad (\text{A7})$$

where we used  $e = 2m_p \mu_N$ . We can find that, in the last expression, the unknown parameters are only  $M_f$ , since  $\mu_f$ ,  $\bar{q}_f$ , and the proton mass  $m_p = 938.27208816$  MeV are already fixed by the experimental values.

For the  $u$  and  $d$  quarks, when we assume the constituent quark masses as  $M_u = M_d = 340$  MeV,

$$a_u = 0.00647922 \rightarrow \kappa_u = 0.00952827 \text{ GeV}^{-1}, \quad (\text{A8})$$

$$a_d = 0.0565187 \rightarrow \kappa_d = 0.0831157 \text{ GeV}^{-1}, \quad (\text{A9})$$

where we used  $\kappa_f \equiv a_f/2M_f$ . These values are consistent with  $\kappa_u = 0.00995 \text{ GeV}^{-1}$  and  $\kappa_d = 0.07975 \text{ GeV}^{-1}$ , which were estimated using  $M_u = M_d = 340$  MeV as Eq. (2.13) of Ref. [50]. We note that, as another estimate in Ref. [50], larger AMMs,  $\kappa_u = 0.29016 \text{ GeV}^{-1}$  and  $\kappa_d = 0.35986 \text{ GeV}^{-1}$ , were obtained in Eq. (2.12) of Ref. [50]. However, its estimate is based on a somewhat larger constituent quark mass  $M_u = M_d = 420$  MeV. Therefore, we discard those values.

For the strange quark, when we assume  $M_s = 550$  MeV,

$$a_s = 0.0779922 \rightarrow \kappa_s = 0.070902 \text{ GeV}^{-1}. \quad (\text{A10})$$

A similar value  $a_s = 0.053$  was obtained in Ref. [55], where  $M_s = 538$  MeV was assumed.

## Appendix B: Dynamical quark mass in the NJL model

In Subsection III D, the masses of constituent quarks under magnetic fields were used as input parameters to quantitatively calculate the Casimir energy. In this Appendix, we briefly explain how to estimate the magnetic-field dependence of dynamical quark masses with AMM. In particular, we use the two-flavor NJL model [94, 95], which is a low-energy effective model with four-point coupling between quarks and useful for investigating the mass generation due to the spontaneous chiral symmetry breaking. For many variations about quarks with AMM under external magnetic field, see Refs. [50–72].

In the NJL model, we assume the mean fields  $(\sigma_u, \sigma_d)$  characterizing the chiral condensates for the up and down quarks and neglect the flavor-mixing effect, such as the  $\sigma_u \sigma_d$  term, for simplicity. The effective potential from the mean-field Lagrangian is written as

$$\begin{aligned} \Omega_{\text{NJL}} = & -N_c \sum_{f=u,d} \frac{|q_f B|}{2\pi} \sum_{s=\pm} \sum_{l=0}^{\infty} \int \frac{dk_z}{2\pi} \omega_{l,s}^{[f]} F_\Lambda \\ & + \frac{1}{4G} \left( \frac{\sigma_u^2}{2} + \frac{\sigma_d^2}{2} \right), \end{aligned} \quad (\text{B1})$$

where the notation is similar to that of Eq. (7).  $N_c = 3$  is the number of colors, and  $G$  is the four-point coupling constant between quarks. The dispersion relations of constituent quarks with AMM  $\kappa_f$  are

$$\omega_{l,s}^{[f]} = \sqrt{k_z^2 + \left( \sqrt{M_f^2 + |q_f B| (2l + 1 - s\zeta)} - s\kappa_f q_f B \right)^2}, \quad (\text{B2})$$

where  $M_f = m_0 + \sigma_f$  is the effective mass with the current quark mass  $m_0$ . For the regularization function  $F_\Lambda$  with a cutoff parameter  $\Lambda$ , we adopt a magnetic-field-dependent Lorentzian-type function [105–107]:

$$F_\Lambda = \frac{\Lambda^{10}}{\Lambda^{10} + \sqrt{k_z^2 + |q_f B| (2l + 1 - s\zeta)}^{10}}. \quad (\text{B3})$$

For the model parameters, we use  $\Lambda = 0.68138 \text{ GeV}$ ,  $G = 1.860/\Lambda^2$ ,  $m_0 = 4.552 \text{ MeV}$  [108]. By minimizing the effective potential (B1) with respect to  $(\sigma_u, \sigma_d)$ , we can determine their values.

In Fig. 10, we show the numerical results for the effective masses,  $M_u$  and  $M_d$ , where we used the AMMs in Eqs. (A8) and (A9). Thus, the mass shift for the up quark is more rapid than that for the down quark due to the difference between their electric charges. The effect of AMM is quite small (within the current parameters), but it contributes to a negative mass shift.

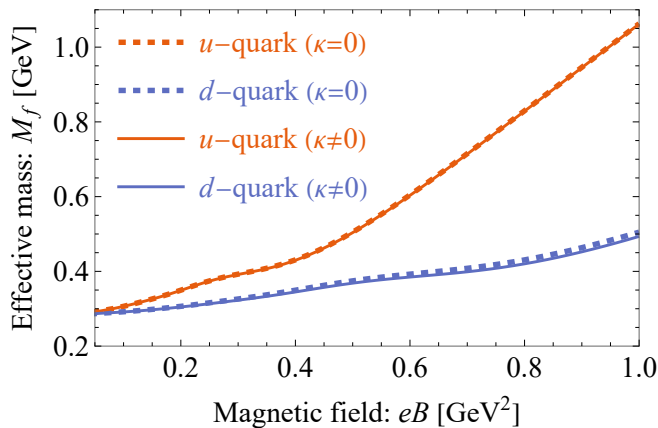


FIG. 10. Magnetic-field dependence of effective masses of the up and down constituent quarks with  $\kappa = 0$  and  $\kappa \neq 0$ .

- 
- [1] H. B. G. Casimir, On the Attraction Between Two Perfectly Conducting Plates, *Proc. Kon. Ned. Akad. Wetensch.* **51**, 793 (1948).
- [2] S. K. Lamoreaux, Demonstration of the Casimir Force in the 0.6 to  $6\mu\text{m}$  Range, *Phys. Rev. Lett.* **78**, 5 (1997), [Erratum: *Phys. Rev. Lett.* **81**, 5475 (1998)].
- [3] G. Bressi, G. Carugno, R. Onofrio, and G. Ruoso, Measurement of the Casimir force between parallel metallic surfaces, *Phys. Rev. Lett.* **88**, 041804 (2002), [arXiv:quant-ph/0203002](#).
- [4] G. Plunien, B. Müller, and W. Greiner, The Casimir Effect, *Phys. Rep.* **134**, 87 (1986).
- [5] V. M. Mostepanenko and N. N. Trunov, The Casimir Effect and Its Applications, *Sov. Phys. Usp.* **31**, 965 (1988).
- [6] M. Bordag, U. Mohideen, and V. M. Mostepanenko, New developments in the Casimir effect, *Phys. Rep.* **353**, 1 (2001), [arXiv:quant-ph/0106045](#) [quant-ph].
- [7] K. A. Milton, *The Casimir Effect: Physical Manifestations of Zero-Point Energy* (World Scientific, Singapore, 2001).
- [8] G. L. Klimchitskaya, U. Mohideen, and V. M. Mostepanenko, The Casimir force between real materials: Experiment and theory, *Rev. Mod. Phys.* **81**, 1827 (2009), [arXiv:0902.4022](#) [cond-mat.other].
- [9] L. M. Woods, D. A. R. Dalvit, A. Tkatchenko, P. Rodriguez-Lopez, A. W. Rodriguez, and R. Podgornik, Materials perspective on Casimir and van der Waals interactions, *Rev. Mod. Phys.* **88**, 045003 (2016), [arXiv:1509.03338](#) [cond-mat.mtrl-sci].
- [10] T. Gong, M. R. Corrado, A. R. Mahbub, C. Shelden, and J. N. Munday, Recent progress in engineering the Casimir effect – applications to nanophotonics, nanomechanics, and chemistry, *Nanophotonics* **10**, 523 (2021).
- [11] B.-S. Lu, The Casimir Effect in Topological Matter, *Universe* **7**, 237 (2021), [arXiv:2105.11059](#) [cond-mat.mes-hall].
- [12] D. Robaschik, K. Scharnhorst, and E. Wieczorek, Radiative corrections to the Casimir pressure under the influence of temperature and external fields, *Annals Phys.* **174**, 401 (1987).
- [13] P. Bruno, Long-range magnetic interaction due to the casimir effect, *Phys. Rev. Lett.* **88**, 240401 (2002), [arXiv:quant-ph/0202006](#) [quant-ph].
- [14] G. Metalidis and P. Bruno, Magnetic casimir effect, *Phys. Rev. A* **66**, 062102 (2002), [arXiv:quant-ph/0207153](#) [quant-ph].
- [15] A. G. Grushin and A. Cortijo, Tunable Casimir Repulsion with Three-Dimensional Topological Insulators, *Phys. Rev. Lett.* **106**, 020403 (2011), [arXiv:1002.3481](#) [cond-mat.mtrl-sci].
- [16] M. V. Cougo-Pinto, C. Farina, M. R. Negro, and A. C. Tort, Bosonic Casimir effect in an external magnetic field, *J. Phys. A* **32**, 4457 (1999), [arXiv:hep-th/9809214](#).
- [17] M. V. Cougo-Pinto, C. Farina, M. R. Negro, and A. C. Tort, Magnetic permeability of constrained scalar QED vacuum, *Phys. Lett. B* **483**, 144 (2000), [arXiv:hep-th/9809216](#).
- [18] M. V. Cougo-Pinto, C. Farina, M. R. Negro, and A. Tort, Casimir effect at finite temperature of charged scalar field in an external magnetic field, (1998), [arXiv:hep-th/9810033](#).
- [19] M. V. Cougo-Pinto, C. Farina, and M. R. Negro, Magnetic properties of confined bosonic vacuum at finite temperature, (1998), [arXiv:hep-th/9811095](#).
- [20] E. Elizalde, F. C. Santos, and A. C. Tort, Confined quantum fields under the influence of a uniform magnetic field, *J. Phys. A* **35**, 7403 (2002), [arXiv:hep-th/0206143](#).
- [21] M. Ostrowski, Casimir effect in external magnetic field, *Acta Phys. Polon. B* **37**, 1753 (2006), [arXiv:hep-th/0504112](#).
- [22] A. Erdas and K. P. Seltzer, Finite temperature Casimir effect for charged massless scalars in a magnetic field, *Phys. Rev. D* **88**, 105007 (2013), [arXiv:1304.6417](#) [hep-th].
- [23] A. Erdas and K. P. Seltzer, Finite temperature Casimir effect for massive scalars in a magnetic field, *Int. J. Mod. Phys. A* **29**, 1450091 (2014), [arXiv:1312.1432](#) [hep-th].
- [24] Y. A. Sitenko and S. A. Yushchenko, The Casimir ef-

- fect with quantized charged scalar matter in background magnetic field, *Int. J. Mod. Phys. A* **29**, 1450052 (2014), [arXiv:1401.6950 \[hep-th\]](#).
- [25] Y. A. Sitenko, Influence of quantized massive matter fields on the Casimir effect, *Mod. Phys. Lett. A* **30**, 1550099 (2015), [arXiv:1506.05034 \[hep-th\]](#).
- [26] A. Erdas, Magnetic field corrections to the repulsive Casimir effect at finite temperature, *Int. J. Mod. Phys. A* **31**, 07 (2016), [arXiv:1511.05940 \[hep-th\]](#).
- [27] A. Erdas, Casimir effect of a Lorentz-violating scalar in magnetic field, *Int. J. Mod. Phys. A* **35**, 2050209 (2020), [arXiv:2005.07830 \[hep-th\]](#).
- [28] S. R. Haridev and P. Samantray, Revisiting vacuum energy in compact spacetimes, *Phys. Lett. B* **835**, 137489 (2022), [arXiv:2106.12171 \[hep-th\]](#).
- [29] A. Erdas, Thermal effects on the Casimir energy of a Lorentz-violating scalar in magnetic field, *Int. J. Mod. Phys. A* **36**, 2150155 (2021), [arXiv:2103.12823 \[hep-th\]](#).
- [30] A. Erdas, Casimir effect of a doubly Lorentz-violating scalar in magnetic field, *Int. J. Mod. Phys. A* **39**, 2450141 (2024), [arXiv:2408.13188 \[hep-th\]](#).
- [31] B. Droguett and C. Bórquez, Casimir effect of rough plates under a magnetic field in Hořava-Lifshitz theory, *Nucl. Phys. B* **1014**, 116878 (2025), [arXiv:2501.05597 \[hep-th\]](#).
- [32] A. Erdas, Magnetic Casimir effect of a Lorentz-violating scalar with higher-order derivatives, *Int. J. Mod. Phys. A* **40**, 2550061 (2025), [arXiv:2503.06829 \[hep-th\]](#).
- [33] M. V. Cougo-Pinto, C. Farina, and A. C. Tort, Fermionic Casimir effect in an external magnetic field, *Conf. Proc. C* **9809142**, 235 (1999), [arXiv:hep-th/9809215](#).
- [34] M. V. Cougo-Pinto, C. Farina, and A. C. Tort, The influence of an external magnetic field on the fermionic Casimir effect, *Braz. J. Phys.* **31**, 84 (2001).
- [35] M. S. R. Miltao and F. A. Farias, The Casimir energy of Dirac field under a general boundary condition using the zeta function method, *Acta Phys. Polon. B* **39**, 1931 (2008).
- [36] Y. A. Sitenko, Casimir effect with quantized charged spinor matter in background magnetic field, *Phys. Rev. D* **91**, 085012 (2015), [arXiv:1411.2460 \[hep-th\]](#).
- [37] Y. A. Sitenko and S. A. Yushchenko, Pressure from the vacuum of confined spinor matter, *Int. J. Mod. Phys. A* **30**, 1550184 (2015), [arXiv:1512.01397 \[hep-th\]](#).
- [38] K. Nakayama and K. Suzuki, Dirac/Weyl-node-induced oscillating Casimir effect, *Phys. Lett. B* **843**, 138017 (2023), [arXiv:2207.14078 \[cond-mat.mes-hall\]](#).
- [39] A. Rohim, A. Romadani, and A. Salim Adam, Casimir effect of Lorentz-violating charged Dirac field in background magnetic field, *Prog. Theor. Exp. Phys.* **2024**, 033B01 (2024), [arXiv:2307.04448 \[hep-th\]](#).
- [40] A. Erdas, Magnetic corrections to the fermionic Casimir effect in Horava-Lifshitz theories, *Int. J. Mod. Phys. A* **38**, 2350117 (2023), [arXiv:2307.06228 \[hep-th\]](#).
- [41] A. Flachi, M. Nitta, S. Takada, and R. Yoshii, Fermion Casimir effect and magnetic Larkin-Ovchinnikov phases, *Phys. Rev. D* **111**, 016003 (2025), [arXiv:2410.18771 \[hep-th\]](#).
- [42] D. Fujii, K. Nakayama, and K. Suzuki, Casimir effect in magnetic dual chiral density waves, (to be published in *Phys. Rev. D*) (2024), [arXiv:2411.11957 \[hep-ph\]](#).
- [43] J. S. Schwinger, On quantum electrodynamics and the magnetic moment of the electron, *Phys. Rev.* **73**, 416 (1948).
- [44] J. S. Schwinger, Quantum electrodynamics. III: The electromagnetic properties of the electron: Radiative corrections to scattering, *Phys. Rev.* **76**, 790 (1949).
- [45] E. J. Ferrer and V. de la Incera, Dynamically Induced Zeeman Effect in Massless QED, *Phys. Rev. Lett.* **102**, 050402 (2009), [arXiv:0807.4744 \[hep-ph\]](#).
- [46] E. J. Ferrer and V. de la Incera, Dynamically Generated Anomalous Magnetic Moment in Massless QED, *Nucl. Phys. B* **824**, 217 (2010), [arXiv:0905.1733 \[hep-ph\]](#).
- [47] J. P. Singh, Anomalous magnetic moment of light quarks and dynamical symmetry breaking, *Phys. Rev. D* **31**, 1097 (1985).
- [48] P. J. A. Bicudo, J. E. F. T. Ribeiro, and R. Fernandes, The Anomalous magnetic moment of quarks, *Phys. Rev. C* **59**, 1107 (1999), [arXiv:hep-ph/9806243](#).
- [49] L. Chang, Y.-X. Liu, and C. D. Roberts, Dressed-quark anomalous magnetic moments, *Phys. Rev. Lett.* **106**, 072001 (2011), [arXiv:1009.3458 \[nucl-th\]](#).
- [50] S. Fayazbakhsh and N. Sadooghi, Anomalous magnetic moment of hot quarks, inverse magnetic catalysis, and reentrance of the chiral symmetry broken phase, *Phys. Rev. D* **90**, 105030 (2014), [arXiv:1408.5457 \[hep-ph\]](#).
- [51] N. Chaudhuri, S. Ghosh, S. Sarkar, and P. Roy, Effect of the anomalous magnetic moment of quarks on the phase structure and mesonic properties in the NJL model, *Phys. Rev. D* **99**, 116025 (2019), [arXiv:1907.03990 \[nucl-th\]](#).
- [52] S. Ghosh, N. Chaudhuri, S. Sarkar, and P. Roy, Effects of the anomalous magnetic moment of quarks on the dilepton production from hot and dense magnetized quark matter using the NJL model, *Phys. Rev. D* **101**, 096002 (2020), [arXiv:2004.09203 \[nucl-th\]](#).
- [53] K. Xu, J. Chao, and M. Huang, Effect of the anomalous magnetic moment of quarks on magnetized QCD matter and meson spectra, *Phys. Rev. D* **103**, 076015 (2021), [arXiv:2007.13122 \[hep-ph\]](#).
- [54] J. Mei and S. Mao, Inverse catalysis effect of the quark anomalous magnetic moment to chiral restoration and deconfinement phase transitions, *Phys. Rev. D* **102**, 114035 (2020), [arXiv:2008.12123 \[hep-ph\]](#).
- [55] R. M. Aguirre, Regularization of the Nambu–Jona-Lasinio model under a uniform magnetic field and the role of the anomalous magnetic moments, *Phys. Rev. D* **102**, 096025 (2020), [arXiv:2009.01828 \[hep-ph\]](#).
- [56] X.-J. Wen, R. He, and J.-B. Liu, Effect of the anomalous magnetic moment on the chiral transition in a strong magnetic field, *Phys. Rev. D* **103**, 094020 (2021).
- [57] R. M. Aguirre, Effects of the anomalous magnetic moments of the quarks on the neutral pion properties within a SU(2) Nambu–Jona Lasinio model, *Eur. Phys. J. A* **57**, 166 (2021), [arXiv:2312.13882 \[hep-ph\]](#).
- [58] N. Chaudhuri, S. Ghosh, S. Sarkar, and P. Roy, Dilepton production from magnetized quark matter with an anomalous magnetic moment of the quarks using a three-flavor PNJL model, *Phys. Rev. D* **103**, 096021 (2021), [arXiv:2104.11425 \[hep-ph\]](#).
- [59] Y. Wang and S. Matsuzaki, Axial inverse magnetic catalysis, *Phys. Rev. D* **105**, 074015 (2022), [arXiv:2110.10432 \[hep-ph\]](#).
- [60] N. Chaudhuri, A. Mukherjee, S. Ghosh, S. Sarkar, and P. Roy, Insignificance of the anomalous magnetic moment of the quarks in presence of chiral imbalance, *Eur. Phys. J. A* **58**, 82 (2022), [arXiv:2111.12058 \[hep-ph\]](#).

- [61] F. Lin, K. Xu, and M. Huang, Magnetism of QCD matter and the pion mass from tensor-type spin polarization and the anomalous magnetic moment of quarks, *Phys. Rev. D* **106**, 016005 (2022), [arXiv:2202.03226 \[hep-ph\]](#).
- [62] M. Kawaguchi and M. Huang, Restriction on the form of the quark anomalous magnetic moment from lattice QCD results, *Chin. Phys. C* **47**, 064103 (2023), [arXiv:2205.08169 \[hep-ph\]](#).
- [63] S. Mao, Inverse catalysis effect of the quark anomalous magnetic moment to chiral restoration and deconfinement phase transitions at finite baryon chemical potential, *Phys. Rev. D* **106**, 034018 (2022), [arXiv:2206.12054 \[nucl-th\]](#).
- [64] X.-L. Sheng, S.-Y. Yang, Y.-L. Zou, and D. Hou, Mass splitting and spin alignment for  $\phi$  mesons in a magnetic field in NJL model, *Eur. Phys. J. C* **84**, 299 (2024), [arXiv:2209.01872 \[nucl-th\]](#).
- [65] N. Chaudhuri, S. Ghosh, P. Roy, and S. Sarkar, Anisotropic pressure of magnetized quark matter with anomalous magnetic moment, *Phys. Rev. D* **106**, 056020 (2022), [arXiv:2209.02248 \[hep-ph\]](#).
- [66] R. He and X.-J. Wen, Effect of anomalous magnetic moment on the chiral transition at zero temperature in a strong magnetic field, *Phys. Rev. D* **106**, 116023 (2022), [arXiv:2212.02787 \[hep-ph\]](#).
- [67] Y.-W. Qiu and S.-Q. Feng, Spin polarization and anomalous magnetic moment in a (2+1)-flavor Nambu–Jona-Lasinio model in a thermomagnetic background, *Phys. Rev. D* **107**, 076004 (2023), [arXiv:2301.01465 \[hep-ph\]](#).
- [68] W. R. Tavares, S. S. Avancini, R. L. S. Farias, and R. P. Cardoso, Artificial first-order phase transition in a magnetized Nambu–Jona-Lasinio model with a quark anomalous magnetic moment, *Phys. Rev. D* **109**, 016011 (2024), [arXiv:2309.04055 \[hep-ph\]](#).
- [69] R. He and X.-J. Wen, Anisotropy and paramagnetism of QCD matter with an anomalous magnetic moment, *J. Phys. G* **51**, 065001 (2024).
- [70] R. Mondal, S. Duari, N. Chaudhuri, S. Sarkar, and P. Roy, Speed of sound and isothermal compressibility in a magnetized quark matter with anomalous magnetic moment of quarks, *Phys. Rev. D* **110**, 054010 (2024), [arXiv:2408.04398 \[hep-ph\]](#).
- [71] M. Kawaguchi, I. Siddique, and M. Huang, Effect of quark anomalous magnetic moment on neutral dense quark matter under magnetic field, *Eur. Phys. J. C* **85**, 246 (2025), [arXiv:2408.14808 \[hep-ph\]](#).
- [72] C.-Y. Yang and S.-Q. Feng, Quark Anomalous Magnetic Moments and Neutral Pseudoscalar Meson Dynamics in Magnetized QCD Matter, (2025), [arXiv:2503.17056 \[hep-ph\]](#).
- [73] E. J. Ferrer, V. de la Incera, I. Portillo, and M. Quiroz, New look at the QCD ground state in a magnetic field, *Phys. Rev. D* **89**, 085034 (2014), [arXiv:1311.3400 \[nucl-th\]](#).
- [74] S. Mao and D. H. Rischke, Dynamically generated magnetic moment in the Wigner-function formalism, *Phys. Lett. B* **792**, 149 (2019), [arXiv:1812.06684 \[hep-th\]](#).
- [75] Y.-R. Bao and S.-Q. Feng, Effects of tensor spin polarization on the chiral restoration and deconfinement phase transitions, *Phys. Rev. D* **109**, 096033 (2024), [arXiv:2403.16541 \[hep-ph\]](#).
- [76] I. M. Ternov, V. G. Bagrov, and V. C. Zhukovsky, Synchrotron radiation of an electron with a vacuum magnetic moment, *Vestnik Mosk. Univ. Fiz. Astron.* **1**, 30 (1966).
- [77] I. I. Rabi, Das freie Elektron im homogenen Magnetfeld nach der Diracschen Theorie, *Z. Phys.* **49**, 507 (1928).
- [78] M. H. Johnson and B. A. Lippmann, Motion in a constant magnetic field, *Phys. Rev.* **76**, 828 (1949).
- [79] R. F. O’Connell, Effect of the Anomalous Magnetic Moment of the Electron on Spontaneous Pair Production in a Strong Magnetic Field, *Phys. Rev. Lett.* **21**, 397 (1968).
- [80] H.-Y. Chiu, V. Canuto, and L. Fassio-Canuto, Quantum theory of an electron gas with anomalous magnetic moments in intense magnetic fields, *Phys. Rev.* **176**, 1438 (1968).
- [81] E. M. Lifshitz, The theory of molecular attractive forces between solids, *Sov. Phys. JETP* **2**, 73 (1956).
- [82] P. Hays, Vacuum fluctuations of a confined massive field in two dimensions, *Ann. Phys. (N.Y.)* **121**, 32 (1979).
- [83] S. G. Mamaev and N. N. Trunov, Vacuum expectation values of the energy-momentum tensor of quantized fields on manifolds with different topologies and geometries. III, *Sov. Phys. J.* **23**, 551 (1980).
- [84] J. Ambjørn and S. Wolfram, Properties of the vacuum. I. Mechanical and thermodynamic, *Ann. Phys. (N.Y.)* **147**, 1 (1983).
- [85] S. Gupta, Magnetic polarizability of the electron, *Nature* **163**, 686 (1949).
- [86] M. Demeur, Etude de l’interaction entre le champ propre d’une particule et un champ électro-magnétique homogène et constant, *Acad. R. Belg., Cl. Sci.* **28**, 1643 (1953).
- [87] R. G. Newton, Radiative effects in a constant field, *Phys. Rev.* **96**, 523 (1954).
- [88] I. M. Ternov, V. G. Bagrov, V. A. Bordovitsyn, and O. Dorofeev, Concerning the Anomalous Magnetic Moment of the Electron, *Zh. Eksp. Teor. Fiz.* **55**, 2273 (1969), [*Sov. Phys. JETP* **28**, 1206 (1969)].
- [89] V. I. Ritus, Radiative Effects and Their Enhancement in an Intense Electromagnetic Field, *Zh. Eksp. Teor. Fiz.* **57**, 2176 (1969), [*Sov. Phys. JETP* **30**, 1181 (1970)].
- [90] B. Jancovici, Radiative correction to the ground-state energy of an electron in an intense magnetic field, *Phys. Rev.* **187**, 2275 (1969).
- [91] W.-Y. Tsai and A. Yildiz, Motion of an electron in a homogeneous magnetic field-modified propagation function and synchrotron radiation, *Phys. Rev. D* **8**, 3446 (1973), [Erratum: *Phys. Rev. D* **9**, 2489 (1974)].
- [92] V. N. Baier, V. M. Katkov, and V. M. Strakhovenko, Anomalous magnetic moment of the electron in the magnetic field, *Yad. Fiz.* **24**, 379 (1976), [*Sov. J. Nucl. Phys.* **24**, 197 (1976), *Lett. Nuovo Cim.* **15**, 149 (1976)].
- [93] S. Navas *et al.* (Particle Data Group), Review of particle physics, *Phys. Rev. D* **110**, 030001 (2024).
- [94] Y. Nambu and G. Jona-Lasinio, Dynamical Model of Elementary Particles Based on an Analogy with Superconductivity. I, *Phys. Rev.* **122**, 345 (1961).
- [95] Y. Nambu and G. Jona-Lasinio, Dynamical Model of Elementary Particles Based on an Analogy with Superconductivity. II, *Phys. Rev.* **124**, 246 (1961).
- [96] M. N. Chernodub, V. A. Goy, A. V. Molochkov, and H. H. Nguyen, Casimir Effect in Yang-Mills Theory in  $D = 2 + 1$ , *Phys. Rev. Lett.* **121**, 191601 (2018), [arXiv:1805.11887 \[hep-lat\]](#).
- [97] M. N. Chernodub, V. A. Goy, and A. V. Molochkov,

- Phase structure of lattice Yang-Mills theory on  $\mathbb{T}^2 \times \mathbb{R}^2$ , *Phys. Rev. D* **99**, 074021 (2019), [arXiv:1811.01550 \[hep-lat\]](#).
- [98] M. Kitazawa, S. Mogliacci, I. Kolbé, and W. A. Horowitz, Anisotropic pressure induced by finite-size effects in SU(3) Yang-Mills theory, *Phys. Rev. D* **99**, 094507 (2019), [arXiv:1904.00241 \[hep-lat\]](#).
- [99] M. N. Chernodub, V. A. Goy, A. V. Molochkov, and A. S. Tanashkin, Boundary states and non-Abelian Casimir effect in lattice Yang-Mills theory, *Phys. Rev. D* **108**, 014515 (2023), [arXiv:2302.00376 \[hep-lat\]](#).
- [100] M. Strickland, V. Dexheimer, and D. P. Menezes, Bulk Properties of a Fermi Gas in a Magnetic Field, *Phys. Rev. D* **86**, 125032 (2012), [arXiv:1209.3276 \[nucl-th\]](#).
- [101] E. J. Ferrer, V. de la Incera, D. Manreza Paret, A. Pérez Martínez, and A. Sanchez, Insignificance of the anomalous magnetic moment of charged fermions for the equation of state of a magnetized and dense medium, *Phys. Rev. D* **91**, 085041 (2015), [arXiv:1501.06616 \[hep-ph\]](#).
- [102] D. Fujii, K. Nakayama, and K. Suzuki, Dual chiral density wave induced oscillating Casimir effect, *Phys. Rev. D* **110**, 014039 (2024), [arXiv:2402.17638 \[hep-ph\]](#).
- [103] D. Fujii, K. Nakayama, and K. Suzuki, Lifshitz formulas for finite-density Casimir effect, (2024), [arXiv:2408.08384 \[quant-ph\]](#).
- [104] J. Franklin, A model of baryons made of quarks with hidden spin, *Phys. Rev.* **172**, 1807 (1968).
- [105] K. Fukushima, M. Ruggieri, and R. Gatto, Chiral magnetic effect in the PNJL model, *Phys. Rev. D* **81**, 114031 (2010), [arXiv:1003.0047 \[hep-ph\]](#).
- [106] R. Gatto and M. Ruggieri, Dressed Polyakov loop and phase diagram of hot quark matter under magnetic field, *Phys. Rev. D* **82**, 054027 (2010), [arXiv:1007.0790 \[hep-ph\]](#).
- [107] R. Gatto and M. Ruggieri, Deconfinement and chiral symmetry restoration in a strong magnetic background, *Phys. Rev. D* **83**, 034016 (2011), [arXiv:1012.1291 \[hep-ph\]](#).
- [108] S. S. Avancini, R. L. S. Farias, N. N. Scoccola, and W. R. Tavares, NJL-type models in the presence of intense magnetic fields: the role of the regularization prescription, *Phys. Rev. D* **99**, 116002 (2019), [arXiv:1904.02730 \[hep-ph\]](#).